The Astrophysical Journal, 878:90 (8pp), 2019 June 20 https://doi.org/10.3847/1538-4357/ab1f93

Detection of 4765 MHz OH Emission in a Preplanetary Nebula: CRL 618

A. Strack[1], E. D. Araya[1], M. E. Lebrón[2], R. F. Minchin[3,4], H. G. Arce[5], T. Ghosh[4,6], P. Hofner[7,11], S. Kurtz[8], L. Olmi[9], Y. Pihlström[10,11], and C. J. Salter[4,6]
[1] Physics Department, Western Illinois University, 1 University Circle, Macomb, IL 61455, USA; ed-araya@wiu.edu
[2] Department of Physical Sciences, University of Puerto Rico, San Juan, PR 00931, USA
[3] USRA, SOFIA, NASA Ames Research Center, Moffett Field, CA 94035, USA
[4] Arecibo Observatory, NAIC, HC3 Box 53995, Arecibo, PR 00612, USA
[5] Department of Astronomy, Yale University, New Haven, CT 06511, USA
[6] Green Bank Observatory, P.O. Box 2, Green Bank, WV 24944, USA
[7] New Mexico Institute of Mining and Technology, Physics Department, 801 Leroy Place, Socorro, NM 87801, USA
[8] Instituto de Radioastronomía y Astrofísica, Universidad Nacional Autónoma de México, Apdo. Postal 3-72, 58089, Morelia, Michoacán, Mexico
[9] INAF, Osservatorio Astrofisico di Arcetri, Largo E. Fermi 5, I-50125 Firenze, Italy
[10] Department of Physics and Astronomy, The University of New Mexico, Albuquerque, NM 87131, USA
Received 2019 March 20; revised 2019 April 25; accepted 2019 April 29; published 2019 June 18

Abstract

Jets and outflows are ubiquitous phenomena in astrophysics, found in our Galaxy in diverse environments, from the formation of stars to late-type stellar objects. We present observations conducted with the 305 m Arecibo Telescope of the preplanetary nebula CRL 618 (Westbrook Nebula)—a well-studied late-type star that has developed bipolar jets. The observations resulted in the first detection of 4765 MHz OH in a late-type stellar object. The line was narrow (FWHM $\sim$ 0.6 km s^{-1}) and $\sim$40 km s^{-1} blueshifted with respect to the systemic velocity, which suggests association with the expanding jets/bullets in CRL 618. We also report nondetection at Arecibo of any other OH transition between 1 and 9 GHz. The nondetections were obtained during the observations in 2008, when the 4765 MHz OH line was first discovered, and also in 2015 when the 4765 MHz OH line was not detected. Our data indicate that the 4765 MHz OH line was a variable maser. Modeling of the 4765 MHz OH detection and nondetection of the other transitions is consistent with the physical conditions expected in CRL 618. The 4765 MHz OH maser could originate from dissociation of H_2O by shocks after sublimation of icy objects in this dying carbon-rich stellar system, although other alternatives such as OH in an oxygen-rich circumstellar region associated with a binary companion are also possible.

Key words: circumstellar matter – masers – stars: AGB and post-AGB – stars: individual (CRL 618)

Supporting material: data behind figure

1. Introduction

The transition from the asymptotic giant branch (AGB) to the planetary nebula (PN) phase is among the most important areas of study in stellar astrophysics today. The post-AGB/preplanetary nebula (PPN) phase occurs when a significant fraction of the stellar mass is ejected within a few thousand years, revealing the core of the star, i.e., a new white dwarf (e.g., Sánchez Contreras et al. 2017; Matthews & Claussen 2018). The PPN phase is when asymmetries develop and grow in the structure of the nebula, resulting in a bipolar morphology. The mechanisms responsible for the development of bipolar asymmetries are under investigation and include the effects of rotation, latitudinal density anisotropy, binarity, and magnetic collimation (e.g., García-Segura et al. 1999, 2014; Blackman et al. 2001). A key probe for the formation and growth of asymmetries has been the study of masers, such as in water fountain objects (e.g., Amiri et al. 2010). Stellar masers of SiO, H_2O, and ground-state OH are commonly detected in oxygen-rich AGB stars, but during the transition to PNe these masers wither away; first SiO, then H_2O, and finally the OH masers disappear (e.g., Habing 1996; Desmurs 2012; Uscanga et al. 2012). At present, only seven PNe have been confirmed to show ground-state OH masers (Uscanga et al. 2012; Qiao et al. 2016).

A prototypical example of a PPN is CRL 618 (IRAS 04395 +3601, V353 Aur, the Westbrook Nebula; Trammell & Goodrich 2002; Cerrigone et al. 2011), which is located at a distance of $\sim$900 pc (Sánchez Contreras et al. 2004; Lee et al. 2013).[12] CRL 618 began its post-AGB phase just over 100 yr ago (Kwok & Feldman 1981; Sánchez Contreras et al. 2004). The central star ($T_{\rm effective}$ $\sim$ 30,000 K) has begun ionization of the envelope in the transition from AGB to the PN phase (e.g., Pardo et al. 2004). Variable radio continuum has been detected in this source, which indicates episodes of expansion of the ionization front in the circumstellar envelope (Kwok & Feldman 1981; Cerrigone et al. 2011). Molecular spectral-line observations have shown evidence for at least two significant episodes of mass loss during the past $\sim$2500 yr (Sánchez Contreras et al. 2004). CRL 618 is characterized by spherical envelopes, jets/outflows, and shocks (bullets), all with different expansion velocities. In particular, it harbors a fast outflow with velocities from 40 to $\sim$300 km s^{-1} (see Figures 5 and 8 in Sánchez Contreras et al. 2004; see also Trammell & Goodrich 2002).

CRL 618 is a carbon-rich object (Herpin et al. 2001), i.e., the progenitor AGB was likely a carbon-rich star similar to IRC +10°216 and not an OH/IR star. It is rich in molecular emission, including some oxygen species, and for which

[11] Adjunct Astronomer at the National Radio Astronomy Observatory, 1003 Lopezville Road, Socorro, NM 87801, USA.

[12] However, a distance of 1.7 kpc has also been used in the literature (Martín-Pintado et al. 1988; Wyrowski et al. 2003).

Table 1
Line Parameters of 4765 MHz OH in CRL 618

Epoch	Chan. Width (km s^{-1})	Rms (mJy)	$S_{\nu,\mathrm{cont}}$ (mJy)	$S_{\nu,\mathrm{OH}}$ (mJy)	V_{LSR} (km s^{-1})	FHWM (km s^{-1})
2008 May[a]	0.19	4.6	27	166 (4)	−59.84 (0.01)	0.56 (0.02)
2008 Oct[b]	0.38	1.5	33	142 (2)	−59.67 (0.01)	0.58 (0.01)
2015 Jan/Feb	0.38	1.4	28	…	…	…
2015 Oct	0.38	1.7	29	…	…	…
2017 Mar	0.38	1.5	…	…	…	…

Notes. 1σ statistical errors from the fit are shown in parentheses.
[a] The spectral line is narrow; the line parameters listed here are before smoothing (see Figure 1, top panel, blue dashed line). If the spectrum is smoothed to the channel width of the 2008 October observations (i.e., $\Delta V = 0.38$ km s^{-1}), then the line parameters from a Gaussian fit are $S_{\nu,\mathrm{OH}} = 145$ (4) mJy, $V_{\mathrm{LSR}} = -59.85$ (0.01) km s^{-1}, FWHM = 0.63 (0.02) km s^{-1}, rms = 2.8 mJy.
[b] An additional weak spectral line (tentative detection, $\gtrsim 3\sigma$ in two consecutive channels) was also present in the bandpass; the peak channel parameters are $S_{\nu,\mathrm{OH}} = 6.6$ mJy, $V_{\mathrm{LSR}} = -39.7$ km s^{-1}.

Bujarrabal et al. (1988) reported the first detection of HCO^+ in a carbon-rich stellar object, as well as transitions of many molecular species including CO, ^{13}CO, CS, SiO, CH_3CN, HC_3N, and HC_5N. CRL 618 was also the first carbon-rich object with detection of H_2CO (Cernicharo et al. 1989).

Regarding the maser environment, Yoon et al. (2014) reported no detection of 22 GHz H_2O and 43 GHz SiO masers. Until our work, hydroxyl (OH) masers had not been detected either: Desmurs et al. (2010) reported no detection of the 6 GHz OH excited lines, while Silverglate et al. (1979) reported no detection of the 1612, 1665, or 1667 MHz OH lines. The absence of masers from oxygen species is not surprising because of the carbon-rich nature of CRL 618. However, using the 305 m Arecibo Telescope, we have detected a narrow line corresponding to the 4765 MHz transition of OH. The detection of this line was a byproduct of a survey for H_2CO masers reported in Araya et al. (2015). In this work we focus on the 4765 MHz OH detection, and present complementary observations also conducted with the Arecibo Telescope.[13]

2. Observations and Data Reduction

Observations of CRL 618 were conducted in 2008, 2015, and 2017 using the Arecibo Telescope. The pointing position was R.A. = $04^h42^m53^s.64$, decl. = $+36°06'53''.4$ (J2000). Channel widths and rms values of the observations are listed in Tables 1 and 2. The following subsections give details of the specific runs.

2.1. 2008 May Observations

The 2008 May observations were conducted as part of a survey for 6 cm H_2CO masers toward low-mass star-forming regions and late-type stellar objects (Araya et al. 2015). In addition to the H_2CO line, we observed the 4660, 4750, and 4765 MHz transitions of OH and detected 4765 MHz OH emission in CRL 618. Observation and calibration details are given in Araya et al. (2015).

2.2. 2008 October Observations

All OH transitions between 1 and 9 GHz were observed with the Arecibo Telescope during 2008 October using the *L*-Band Wide, *C*-Band, *C*-Band High, and *X*-Band receivers. The WAPP backend was configured to channel widths between 0.2 and 0.4 km s^{-1} for all the observed bands. The observations were made in position-switched mode. The ON-source integration time per scan was 5 minutes, and three scans were typically obtained per frequency setting. After checking the ON- and OFF-source spectra to search for radio frequency interference (RFI) and signal in the reference position, the spectra were calibrated to flux density units (Jy) using the Arecibo AOIDL package. The orthogonal polarizations were averaged to reduce the noise of the spectra, and the line parameters were measured in cases of detection.

2.3. 2015 January, February, and October Observations

The 2015 observations were made to check for variability of the 2008 detection. In addition, all other OH transitions between 1 and 9 GHz were re-observed with the Arecibo Telescope using the *L*-Band Wide, *C*-Band, *C*-Band High, and *X*-Band receivers. The observations were conducted with the WAPP backend, using channel widths between 0.1 and 0.3 km s^{-1} and bandwidths between 1.56 MHz (*L*-Band) and 6.25 MHz (*X*-Band). Single 5 minute ON-source scans were typically conducted; multiple scans of some spectral windows were obtained to improve sensitivity. Spectra were checked for RFI and calibrated using the Arecibo AOIDL libraries. Polarizations were averaged to reduce the noise of the spectra.

2.4. 2017 March Observations

Further monitoring observations of *C*-Band OH transitions (4660, 4750, and 4765 MHz) were conducted in 2017 March. The observations were carried out in position-switched mode (5 minute ON-source integration time); five scans were obtained. The WAPP backend was used to observe the three OH lines simultaneously with a bandwidth of 3.12 MHz and 2048 channels in dual linear polarization. The data were calibrated in IDL using the Arecibo AOIDL package. The individual polarizations and scans were inspected for consistency (no polarized signal was detected) and to check for RFI, and were then averaged. The 4765 MHz OH spectrum was smoothed to a channel width of 0.38 km s^{-1} (to match the channel width of the 2008 October observations).

3. Results

The 4765 MHz OH line in CRL 618, obtained as part of an H_2CO maser survey by Araya et al. (2015), is the first detection

[13] An initial report of this work (Strack et al. 2018) was published in the proceedings of the IAU 336 Symposium—Astrophysical Masers: Unlocking the Mysteries of the Universe.

Table 2
Upper Limits of Other OH Transitions

Rest Freq. (MHz)	Transition	E_u (K)	Epoch	Chan. Width (km s^{-1})	rms (mJy)
1612.2310	$^2\Pi_{3/2}\,J = 3/2\,F = 1 - 2$	0.080	2015 Feb	0.14	3.9
			2008 Oct	0.28	3.2
1665.4018	$^2\Pi_{3/2}\,J = 3/2\,F = 1 - 1$	0.080	2015 Feb	0.13	3.4
			2008 Oct	0.28	3.1
1667.3590	$^2\Pi_{3/2}\,J = 3/2\,F = 2 - 2$	0.083	2015 Feb	0.13	3.3
			2008 Oct	0.28	3.1
1720.5300	$^2\Pi_{3/2}\,J = 3/2\,F = 2 - 1$	0.083	2015 Feb	0.13	3.3
			2008 Oct	0.27	3.2
4660.2420	$^2\Pi_{1/2}\,J = 1/2\,F = 0 - 1$	181.9	2008 May	0.20	4.4
			2008 Oct	0.39	2.2
			2015 Jan/Feb	0.19	2.7
			2015 Oct	0.19	2.1
			2017 Mar	0.19	1.9
4750.6560	$^2\Pi_{1/2}\,J = 1/2\,F = 1 - 1$	181.9	2008 May	0.19	4.6
			2008 Oct	0.39	1.8
			2015 Jan/Feb	0.19	2.7
			2015 Oct	0.19	2.2
			2017 Mar	0.19	1.9
6016.7460	$^2\Pi_{3/2}\,J = 5/2\,F = 2 - 3$	120.8	2008 Oct	0.30	2.7
			2015 Jan	0.23	14
6030.7483	$^2\Pi_{3/2}\,J = 5/2\,F = 2 - 2$	120.8	2008 Oct	0.30	2.7
			2015 Jan	0.23	10
6035.0934	$^2\Pi_{3/2}\,J = 5/2\,F = 3 - 3$	120.8	2008 Oct	0.30	2.7
			2015 Jan	0.23	9.5
6049.0840	$^2\Pi_{3/2}\,J = 5/2\,F = 3 - 2$	120.8	2008 Oct	0.30	2.7
			2015 Jan	0.23	10
7749.9134	$^2\Pi_{1/2}\,J = 3/2\,F = 1 - 2$	270.1	2008 Oct	0.24	3.4
			2015 Jan	0.24	18
7761.7470	$^2\Pi_{1/2}\,J = 3/2\,F = 1 - 1$	270.1	2008 Oct	0.24	3.9
			2015 Jan	0.24	14
7820.1250	$^2\Pi_{1/2}\,J = 3/2\,F = 2 - 2$	270.1	2008 Oct	0.23	3.5
			2015 Jan	0.23	8.4
7831.9552	$^2\Pi_{1/2}\,J = 3/2\,F = 2 - 1$	270.1	2008 Oct	0.23	3.5
			2015 Jan	0.23	11
8118.0567	$^2\Pi_{1/2}\,J = 5/2\,F = 2 - 3$	415.9	2008 Oct	0.23	3.8
			2015 Jan	0.22	16
8135.8649	$^2\Pi_{1/2}\,J = 5/2\,F = 2 - 2$	415.9	2008 Oct	0.22	3.8
			2015 Jan	0.22	14
8189.5856	$^2\Pi_{1/2}\,J = 5/2\,F = 3 - 3$	415.9	2008 Oct	0.22	4.5
			2015 Jan	0.22	12
8207.3939	$^2\Pi_{1/2}\,J = 5/2\,F = 3 - 2$	415.9	2008 Oct	0.22	3.9
			2015 Jan	0.22	12
8503.1503	$^2\Pi_{1/2}\,J = 11/2\,F = 5 - 6$	1186.7	2008 Oct	0.22	4.4
			2015 Jan	0.21	9.6
8534.8375	$^2\Pi_{1/2}\,J = 11/2\,F = 6 - 6$	1186.7	2008 Oct	0.21	4.7
			2015 Jan	0.21	9.3
8580.1304	$^2\Pi_{1/2}\,J = 11/2\,F = 5 - 5$	1186.7	2008 Oct	0.21	4.8
			2015 Jan	0.21	15
8611.8176	$^2\Pi_{1/2}\,J = 11/2\,F = 6 - 5$	1186.7	2008 Oct	0.21	4.7
			2015 Jan	0.21	15

Note. Spectra were smoothed to the channel width listed in the fifth column. Spectroscopy information from *Splatalogue* (http://www.cv.nrao.edu/php/splat/) and the NIST Lovas catalog (https://physics.nist.gov/cgi-bin/micro/table5/start.pl); see also Pihlström et al. (2008).

of this transition in a late-type stellar object. The 4765 MHz line corresponds to the transition $^2\Pi_{1/2}\,J = 1/2\,F = 1 - 0$ ($E_u = 181.94$ K),[14] which is analogous to the 1720 MHz OH ground-state line but in the $^2\Pi_{1/2}$ ladder instead of the $^2\Pi_{3/2}$ (e.g., Pihlström et al. 2008; see also Figure 5.2 in Gray 2012).

[14] Spectroscopy information from *Splatalogue* (http://www.cv.nrao.edu/php/splat/).

The emission was first detected in the 2008 May observations (Araya et al. 2015), and then confirmed in 2008 October. Figure 1 shows the 4765 MHz OH spectra from 2008 May and October, 2015 January and February, and 2017 March. Both the 2008 May and October observations showed a detection of 4765 MHz OH emission at $V_{\rm LSR} \sim -60$ km s^{-1}. The 2008 May observations were conducted with higher spectral

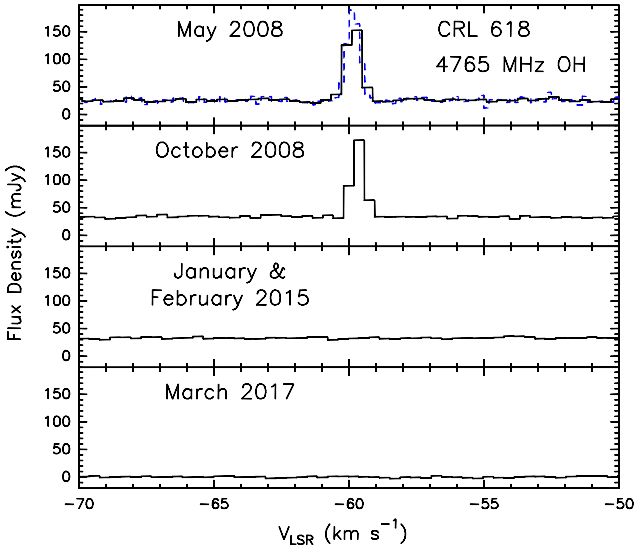

Figure 1. First detection (top panel) and confirmation (middle panel) of 4765 MHz OH emission in a late-type stellar object. The 2008 May observations were conducted with greater spectral resolution than the 2008 October observations. In the top panel, the blue dashed line shows the high spectral resolution data, which were smoothed to generate the spectrum shown in black. The spectral line was not detected in 2015 or 2017. Note the detection of radio continuum from the baseline in 2008 and 2015; as mentioned in Section 3, the 2017 spectrum is shown after baseline subtraction. ASCII files of the spectra shown in this figure (before smoothing). The data used to create this figure are available.

resolution than the 2008 October observations; the high-resolution (non-smoothed) 2008 May spectrum is shown as a blue dashed line in the top panel of Figure 1. The line parameters of the 4765 MHz OH line are listed in Table 1. Table 2 lists the upper limits of the other OH transitions that were observed, including the rms noise values, and the channel widths for each of the upper limits. No emission was detected for any of these other OH transitions.

As shown in Figure 1 and Table 1, we detected radio continuum toward CRL 618 from the baseline level of the (ON–OFF)/OFF spectra from 2008 and 2015. The 2017 observations were conducted at sunset, which was likely responsible for changes in the baseline levels between the ON- and OFF-source observations, and radio continuum was not reliably measured at that epoch (the 2017 spectrum in Figure 1 is shown after baseline subtraction).

4. Discussion

4.1. A 4765 MHz OH Maser in a Carbon-rich Late-type Star: Detection and Variability

OH masers had not been detected in CRL 618 until our 2008 May observations. The detection was confirmed in 2008 October (Figure 1). At both epochs the signal was only seen in the ON-source position and in both polarizations, leading us to rule out RFI. We find it unlikely that the emission is coming from an unrelated object, as CRL 618 is the only IRAS source within the beam and main sidelobes. Arecibo has the smallest half-power beamwidth (HPBW) of all single-dish radio telescopes currently available at 5 GHz (HPBW$_{5\ \mathrm{GHz}} \approx 1'$), and false positives due to nearby sources should not be a problem. This is in contrast to smaller single-dish telescopes, such as the false-positive detection of ground-state OH emission in the carbon star V1187 Ori as demonstrated by observations using the Nançay and Toruń telescopes (Szczerba et al. 2002). The flux density of the 2008 May and October spectral lines were similar (see Table 1). However, the 4765 MHz OH line was not detected in the 2015 and 2017 observations. Given the narrow line width[15] (Table 1), lack of detection of other OH transitions (Table 2), and variability, we can rule out a thermal origin for the line. The flux density of the OH line reported here is similar to the 1665 and 1667 MHz OH maser lines detected toward the silicate carbon star V778 Cyg of about 100 mJy (Little-Marenin et al. 1988; Little-Marenin et al. 1994).

Significant variability of both circumstellar and interstellar masers is a well-known phenomenon (e.g., te Lintel Hekkert & Chapman 1996; Araya et al. 2010). Some circumstellar maser flares of ground-state OH transitions have been observed to last from a few months to several years (e.g., Etoka & Le Squeren 1997; Etoka et al. 2017). The highly variable and rare 4765 MHz OH maser reported in this work is similar to the 1720 MHz OH maser detected toward the young PN K 3-35 (Gómez et al. 2009),[16] which is one of only three known cases of 1720 MHz OH masers in PNe (Gómez et al. 2016; Qiao et al. 2016). The flux density of the 1720 MHz OH maser in K 3-35 decreased from 3 Jy in 1988 (te Lintel Hekkert 1991, see their Figure 1o) to 0.6 Jy by 2002 (Gómez et al. 2009). As in the case of the 4765 MHz OH maser in CRL 618, the single-dish spectrum of the 1720 MHz OH maser in K 3-35 is dominated by a single narrow line.

In the case of carbon-rich objects, H_2O masers in silicate carbon stars are also highly variable. For example, the H_2O maser in NC 83 has shown variability by a factor of more than 40, from nondetections in the 1980s and 1990s, to a 4.1 Jy line in 2007 (Ohnaka et al. 2013). Another example is the silicate carbon star EU And, where Little-Marenin et al. (1988) and Benson & Little-Marenin (1987) reported the detection of a 22 GHz H_2O maser redshifted by 24 km s^{-1} with respect to the systemic velocity (see also Engels 1994). This maser was variable (undetectable at some epochs; Nakada et al. 1987; Little-Marenin et al. 1988) and its spectrum was dominated by a single narrow (FWHM = 0.6 km s^{-1}) line, i.e., similar to the OH maser reported in the present work. Variability of HCN masers in carbon stars (including masers that disappeared within tens of days to several months after detection) has also been detected in other sources (e.g., Lucas et al. 1988; Izumiura et al. 1995; Schilke & Menten 2003).

The LSR velocity of the 4765 MHz OH line reported here is approximately −60 km s^{-1}, and the systemic velocity of the star is −21.5 km s^{-1} (Sánchez Contreras et al. 2004). Thus, the line is blueshifted by ∼40 km s^{-1}. Given our detection and the radial velocity profiles discussed by Sánchez Contreras et al. (2004), the maser could be associated with the interface between the fast bipolar outflow and the dense core region (see their Figure 5; also Figure 11 in Lee et al. 2013). Cernicharo et al. (1989) reported a terminal velocity outflow of ≈200 km s^{-1} based on CO observations, and detected an HC_3N absorption feature at −57.5 km s^{-1} (i.e., very similar to the 4765 MHz OH velocity). They

[15] Note, e.g., that the HC_3N thermal lines in CRL 618 discussed by Wyrowski et al. (2003) are broader than 2 km s^{-1}.

[16] The nature of K3-35 was called into question by Engels et al. (1985); although it is widely accepted to be a young PN, e.g., Miranda et al. (1998).

interpreted this high-velocity feature as tracing absorption against the central radio continuum region.

High-velocity lines have been detected in other post-AGB objects with bipolar asymmetries. For instance, early work by te Lintel Hekkert et al. (1988) reported examples of highly evolved AGB stars with main line OH transitions detected over a broad velocity range ($\gtrsim$100 km s^{-1}), including the water fountain IRAS 16342−3814 (Likkel & Morris 1988), which has shown flux density variability over time periods as short as months with minimal shifts in velocity ($\lesssim$1 km s^{-1}; Likkel et al. 1992). Likewise, in the case of CRL 618, the LSR peak velocity of the two detections agree within 1 km s^{-1} (see Table 1). In the case of the prototypical carbon star IRC+10° 216, a narrow (FWHM $\sim$ 0.3 km s^{-1}) SiS maser line was also detected, blueshifted with respect to the systemic velocity, albeit by a smaller amount (13.5 km s^{-1}; Nguyen-Q-Rieu et al. 1984, assuming a systemic velocity of −26.5 km s^{-1}). Nguyen-Q-Rieu et al. (1984) reported a ∼40% variability of the SiS ($J = 1 - 0$) maser over a period of 10 months. Preferentially blueshifted emission with respect to systemic velocity has also been reported in ground-state OH masers associated with PNe (Uscanga et al. 2012).

An analogous system to CRL 618 is the bipolar PPN object IRAS 08005−2356 (Sahai & Patel 2015), where 1612 MHz OH masers have been detected (te Lintel Hekkert et al. 1991) and there is evidence for dual carbon and oxygen chemistry (Bakker et al. 1997). The 1612 MHz OH masers in IRAS 08005−2356 are blueshifted from the systemic velocity by ∼50 km s^{-1} (Slijkhuis et al. 1991; te Lintel Hekkert et al. 1991). IRAS 07027−7934 is yet another example of a carbon-rich young PN with a 1612 MHz OH maser, which may have transformed from an OH/IR star into a carbon star within the past few hundred years (Zijlstra et al. 1991).

Excited OH lines in late-type stellar objects are extremely rare (Habing 1996). The only confirmed masers are toward the PPNe Vy 2-2 and K 3-35 at 6035 MHz (variable masers; Desmurs et al. 2010). Two other unconfirmed detections were possible artifacts (AU Gem, 4750 MHz OH) or highly variable masers (NML Cyg, 6030 and 6035 MHz; Sjouwerman et al. 2007 and references therein). In the case of Vy 2-2, the OH line is also significantly blueshifted (∼20 km s^{-1} with respect to systemic; Desmurs et al. 2002). We note that 6 cm excited OH lines were not detected in our Arecibo spectral-line survey of IRC+10°216 (Araya et al. 2003).

In summary, although excited OH lines in late-type stellar objects are rare, the overall characteristics of our detection (narrow line, low flux density, variability, blueshifted line with respect to the systemic velocity) are similar to other masers in late-type stellar objects.

4.2. Radio Continuum

Tafoya et al. (2013) reported long-term monitoring observations of the radio continuum in CRL 618 at 5 and 22 GHz. They found an increase in the 5 GHz radio continuum flux density from 6 ± 3 mJy in 1974 to 33 ± 2 mJy in 1998, which they characterized by a +0.8 power law ($S_\nu \propto (t - t_0)^{0.8}$). The 22 GHz continuum variability was also well fit by a +0.8 power law (data between 1982 and 2007). They also found that the angular size of the ionized region monotonically increased and estimated that the circumstellar ionization began in the early 1970s by extrapolating to zero angular size. As shown in Table 1, we detected approximately the same 5 GHz flux density as that measured in the 1990s. This suggests that the 5 GHz radio continuum flux density from the ionized gas in this young PPN remained approximately constant between 1998 and 2015, although the +0.8 power-law flux density increase is still consistent with our measurement within the uncertainty from the fit reported in Equation (1) of Tafoya et al. (2013). Further Arecibo and Very Large Array (VLA) observations are needed to investigate whether the 5 GHz radio continuum has changed since then. We note that according to Wyrowski et al. (2003), the VLA radio continuum observations of CRL 618 are not significantly affected by resolved out extended structure.

4.3. Maser Excitation

We used the 1D radiative transfer code `Molpop` (Elitzur & Asensio Ramos 2006) to check whether it is theoretically possible to have realistic physical conditions for which the 4765 MHz OH transition is inverted while the other transitions observed in this work are not (see Table 2). `Molpop` has the option of invoking the escape probability approximation for the solution of multilevel radiative transfer problems using a plane-parallel slab approximation. We explored a broad parameter space of densities between 10^1 and 10^{10} cm^{-3}, gas temperatures between 50 and 450 K, radiation field from dust at temperatures between 50 and 200 K, and line overlapping excitation with a line width of 1 or 12 km s^{-1}. As an example, Figure 2 shows the results of models assuming a radiation field from warm dust at 150 K, dust $\tau_V = 100$ (Wyrowski et al. 2003), and including line overlapping excitation with a line width of 12 km s^{-1}. The top panel shows the excitation temperature of the 4765 MHz OH transition within a subrange of densities and gas temperatures, and the bottom panel shows the excitation temperature as a function of OH column density for a gas temperature of 315 K and density of 2.5 × 10^6 cm^{-3}. This model predicts population inversion (negative excitation temperature) of only the 4765 MHz OH transition at an OH column density per unit line width of ∼6 × 10^{14} cm^{-2}/(km s^{-1}). Other values for the model parameters (e.g., a gas temperature of 158 K, number density of 5 × 10^6 cm^{-3}, and OH column density per unit line width of ∼8 × 10^{14} cm^{-2}/(km s^{-1})) also result in inversion of the 4765 MHz OH energy states, while other transitions show weak or no inversion. Given that the maser was not imaged (its angular size and location with respect to the continuum source are unknown), no attempt was made to model the flux density or brightness temperature of the maser based on the inversion level; our intent is to simply explore whether the 4765 MHz OH transition can be inverted while the other transitions are not. We note that similar models developed for star-forming environments (Pavlakis & Kylafis 1996; Cragg et al. 2002; Ellingsen et al. 2004) also predict that specific physical conditions can lead the 4765 MHz OH transition to be a dominant maser line with large brightness temperatures (>10^4 K).

The conditions used for the model shown in Figure 2 are reasonable based on the complex environment of CRL 618. The rotation temperatures derived from HC_3N and HC_5N transitions range from 80 to 670 K (Bujarrabal et al. 1988), which encompass the gas temperature of 315 K used in the model. A temperature of ∼300 K was also assumed in the model of Pardo et al. (2004) for the slowly expanding molecular gas region at the base of the high-velocity wind

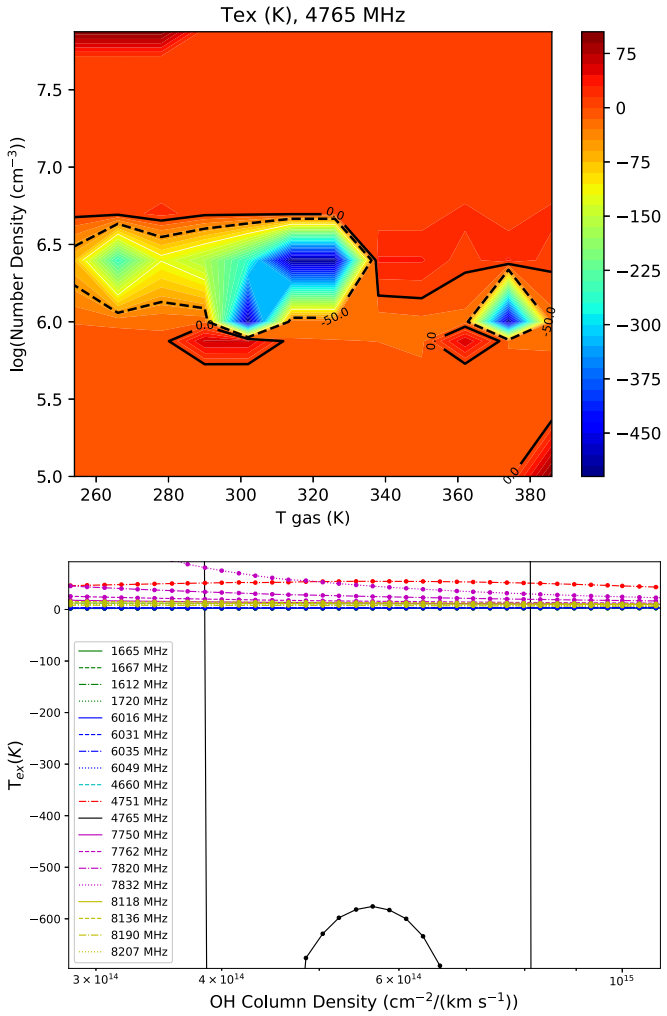

Figure 2. Radiative transfer model of OH transitions observed in this work using the code `Molpop` (Elitzur & Asensio Ramos 2006). Top panel shows the excitation temperature of the 4765 MHz OH transition as a function of molecular density and gas temperature. Bottom panel shows that inversion of the 4765 MHz OH line, but not the other transitions, is possible under specific physical conditions (see Section 4.3). The vertical lines mark the range of specific column densities where the 4765 MHz OH transition is inverted for a given set of physical parameters (Section 4.3). The asymptotically negative excitation temperature values approaching the vertical lines mark the transition to noninverted states where the maser action disappears (e.g., see Figure 7 of Thaddeus 1972).

(see their Figure 4). Also, the chemical structure model presented by Herpin & Cernicharo (2000, e.g., see their Figure 3) locates the OH-rich region inside the high-velocity wind region at a temperature of ∼250 K. Silverglate et al. (1979) reported an upper limit of 8.6×10^{16} cm^{-2} for the OH column density in CRL 618, which is consistent with the column density needed for inversion shown in Figure 2. Herpin & Cernicharo (2000) report an OH column density of 8×10^{15} cm^{-2}, which is also similar to the one from Figure 2 (note that the abscissa is in units of column density per unit line width). The line width of 12 km s^{-1} assumed for the line-overlap effect is also possible; e.g., Lee et al. (2013) reported multiple molecular transitions with line widths $\geqslant$10 km s^{-1} (see their Figure 9). Martín-Pintado et al. (1988) modeled the IR SED of CRL 618 as the superposition of two blackbodies with temperatures of 95 and 280 K, which encompass the dust temperature of 150 K used to generate Figure 2. We note that the slowly expanding (∼20 km s^{-1}) and relatively cold (30–100 K) gas+dust envelope discussed by Cernicharo et al. (1989) could also contribute to the IR field responsible for the excitation. The density assumed in Figure 2 (2.5×10^6 cm^{-3}) is similar to the density of the high-velocity wind region (10^5–10^6 cm^{-3}) and the density of the ∼20 km s^{-1} expanding molecular torus (∼10^7 cm^{-3}) reported by Herpin & Cernicharo (2000). Thus, from a theoretical perspective, physical conditions in environments similar to those expected in CRL 618 can lead the 4765 MHz OH transition to be inverted.

As mentioned above, the 4765 MHz OH detection is blueshifted by ∼40 km s^{-1} with respect to the systemic velocity, and there is evidence that the OH gas traces the inner circumstellar envelope (Herpin & Cernicharo 2000). Thus, the maser is likely located in the foreground of the radio continuum source. This is similar to the case of the very young PN K3-35 where the 1667 and 1612 MHz OH masers are blueshifted with respect to the systemic velocity by ∼20 km s^{-1} (Gómez et al. 2009). Given the variability of the 4765 MHz OH maser in CRL 618, it is likely that the maser was unsaturated, i.e., exponential growth of flux density with distance through the medium by amplifying the background radio continuum (e.g., Gray 2012). However, a reliable estimate of the maser gain is not possible because of the uncertain location of the maser with respect to the background radio continuum. The characteristics of the OH maser in CRL 618 are similar to other masers in carbon-rich objects. For example, the HCN (1–0) maser in Y CVn was modeled by Dinh-V-Trung & Rieu (2000) as unsaturated emission (consistent with a high level of variability) and $T_{\rm ex} < -100$ K.

4.4. Scenarios for the Origin of the 4765 MHz OH Maser in CRL 618

In OH/IR stars it is thought that OH is produced through photodissociation of H_2O (e.g., Habing 1996). In some cases, 1665 and 1667 MHz OH masers have been found located in regions where H_2O masers originate. For instance, Richards et al. (2011) studied U Ori and U Her that have shown OH and H_2O maser variability and where the OH masers may originate from the inner circumstellar envelope (Etoka & Le Squeren 1997). In the case of CRL 618, Herpin & Cernicharo (2000) detected H_2O and OH transitions at far-IR wavelengths. Herpin & Cernicharo (2000) discussed the possibility that OH could be produced through the photodissociation of CO and recombination of molecules. The OH and H_2O produced via this process occupy the innermost molecular envelope where the UV flux is the strongest. Other possible mechanisms that may contribute to the production of OH are shock-induced chemistry and photodissociation of H_2O in the interface between the ionized region and the circumstellar gas, which is pushed at high speeds in the outflow (note that Tafoya et al. 2013 reported expansion of the ionized region in CRL 618). Cernicharo et al. (1989) pointed out that OH and other molecules can reform after ∼1 yr in post-shocked gas (see also Neufeld & Dalgarno 1989); thus, significant velocity shifts with respect to systemic would be expected, as in the case of our detection.

The likely association of the OH maser gas with H_2O is also strengthened by the case of the young PN K3-35, where Gómez et al. (2009) reported detection of masers from the four ground-state OH lines. They found 1720 MHz masers to have very similar velocity and location to the H_2O masers. An excited OH

maser of the 6035 MHz transition has also been detected toward K3-35, and, as for the 1720 MHz OH masers, the excited OH maser in K3-35 is coincident in position and velocity with H_2O masers and may originate from the inner circumstellar envelope (Gómez et al. 2009; Desmurs et al. 2010).

According to the model by Herpin & Cernicharo (2000), the region where OH and H_2O are located in CRL 618 is within 1400 au of the star. In our solar system, that volume includes the Kuiper Belt and the inner Oort Cloud where countless icy objects are found. We point out that in the carbon-rich environment of CRL 618, a source of H_2O could be sublimation from icy objects in its Kuiper Belt/Oort Cloud; H_2O could then be dissociated to form the OH molecules required for the maser. As pointed out by Stern et al. (1990) and Melnick et al. (2001), H_2O from icy objects around an AGB star may be directly sublimated by the thermal radiation of the star up to several hundred astronomical units away from the central source, and thus icy objects much farther away (in an analog Oort Cloud) would not be a source of H_2O vapor if only thermal sublimation is considered. Instead, taking into account the significant velocity difference between the maser emission and the systemic velocity, shocks interacting with the icy objects in the outflow could be responsible for the sublimation. As demonstrated by the ESA *Rosetta* mission to comet 67P/Churyumov–Gerasimenko, outgassing in a comet can result in H_2O column densities between 10^{14} and 10^{16} cm^{-2} (Marschall et al. 2016), i.e., similar to the OH column density required by our model. Thus, the detection of the short-lived 4765 MHz OH maser reported in this work may not only be tracing the end of the star's life in its transition to a PN, but also the destruction of icy objects that have existed since the formation of the star.

CRL 618 is a more-evolved example of systems similar to the carbon star IRC+10°216, as CRL 618 has a greater effective temperature (~32,000 K; Tafoya et al. 2013 and references therein) than IRC+10°216 (~2200 K; e.g., Matthews & Reid 2007), and CRL 618 shows strong radio continuum emission from ionized gas as the star transitions to a PN (e.g., Tafoya et al. 2013; the radio continuum in IRC +10°216 is significantly weaker, see Dinh-V-Trung & Lim 2008). Melnick et al. (2001) reported detection of a 556.9 GHz H_2O transition in IRC+10°216 and interpreted this detection as evidence for sublimation of H_2O from orbiting comets. Ford et al. (2003) later detected 1665 and 1667 MHz OH lines using the Arecibo Telescope (the OH lines in IRC +10°216 are blueshifted by ~10 km s^{-1} with respect to the systemic velocity). As pointed out by Ford et al. (2003 and references therein), OH in IRC+10°216 could also originate from sublimation of icy objects in a Kuiper Belt analog (an extrasolar cometary system).

The idea of destruction of icy objects has also been proposed as the source of OH in silicate carbon stars with OH ground-state maser detections (e.g., Szczerba et al. 2007). Other scenarios proposed to explain ground-state OH masers in silicate carbon stars include the presence of an oxygen-rich envelope ejected before the carbon enrichment during the thermal pulses and dredge-up, or an oxygen-rich disk around a companion star (Szczerba et al. 2007). Indeed, water masers in silicate carbon stars are thought to originate in an oxygen-rich circumbinary or circumstellar disk around a low-luminosity companion of the carbon star (a white dwarf or main-sequence star; e.g., see Benson & Little-Marenin 1987; Little-Marenin et al. 1988; Szczerba et al. 2006; Ohnaka et al. 2013; although a white dwarf companion may be less likely, see Deguchi et al. 1988). Cernicharo et al. (1989) mentioned that the bipolar outflow in CRL 618 could be caused by a close binary, and Tafoya et al. (2013) also discussed the possibility of a binary system based in part on the morphology of the radio continuum. Thus, the OH maser in CRL 618 could have originated instead from an oxygen-rich region similar to those proposed for silicate carbon stars (e.g., Ohnaka et al. 2013).

5. Concluding Remarks

We report high-sensitivity observations conducted with the 305 m Arecibo Telescope spread over a decade of the 4765 MHz OH line in CRL 618. The line was detected in two independent observing runs in 2008. However, it was not detected in either 2015 or 2017. This is the first detection of the 4765 MHz OH transition in a late-type stellar object, and is a particularly interesting result because CRL 618 is a carbon-rich PPN. Using Arecibo, we observed all other OH transitions between 1 and 9 GHz, but detected no other OH line. Observations of the other transitions were conducted when the 4765 MHz OH line was detected (in 2008) and when that line was not detected (in 2015). The narrow line width of the 4765 MHz OH line (0.6 km s^{-1}), the absence of other OH transitions, the large velocity difference (~40 km s^{-1} blueshifted) between the line and the systemic velocity of the star, and its large variability indicate that the 4765 MHz OH line was a maser.

Using the radiative transfer code `Molpop` (Elitzur & Asensio Ramos 2006), we find that inversion of the 4765 MHz OH line (and the absence of all other OH transitions between 1 and 9 GHz) can be explained assuming reasonable physical conditions for a PPN environment. We propose that the OH may originate from sublimation of H_2O molecules from icy objects in the Kuiper Belt/Oort Cloud analogous region of CRL 618, followed by molecular dissociation by UV radiation or shocks. Further monitoring of the 4765 MHz OH transition in CRL 618 and other PPNe is required to investigate how common this line is in PPN objects. If this transition traces the inner regions of PPNe, VLBI observations could be used to investigate the development of bipolar structures.

We thank an anonymous referee for comments that improved the manuscript. A.S. and E.D.A. acknowledge the support of WIU Distinguished Alumnus Frank Rodeffer to the WIU Physics Department and the WIU Astrophysics Research Laboratory, in particular student scholarships and computational resources. E.D.A. acknowledges partial support from NSF grant AST-1814063. P.H. acknowledges partial support from NSF grant AST-1814011. Until 2018 March 31, the Arecibo Observatory was operated by SRI International under a cooperative agreement with the National Science Foundation (AST-1100968), and in alliance with Ana G. Méndez-Universidad Metropolitana, and the Universities Space Research Association. This research has made use of NASA's Astrophysics Data System; the SIMBAD database, operated at CDS, Strasbourg, France; and the NASA/IPAC Infrared Science Archive, which is operated by the Jet Propulsion Laboratory, California Institute of Technology, under contract with the National Aeronautics and Space Administration.

Software: AOIDL, Molpop (Elitzur & Asensio Ramos 2006).

ORCID iDs

E. D. Araya https://orcid.org/0000-0001-6755-9106
R. F. Minchin https://orcid.org/0000-0002-1261-6641
H. G. Arce https://orcid.org/0000-0001-5653-7817
T. Ghosh https://orcid.org/0000-0003-4454-2875
L. Olmi https://orcid.org/0000-0002-1162-7947
Y. Pihlström https://orcid.org/0000-0003-0615-1785

References

Amiri, N., Vlemmings, W., & van Langevelde, H. J. 2010, A&A, 509, A26
Araya, E., Hofner, P., Goldsmith, P., Slysh, S., & Takano, S. 2003, ApJ, 596, 556
Araya, E. D., Hofner, P., Goss, W. M., et al. 2010, ApJL, 717, L133
Araya, E. D., Olmi, L., Morales Ortiz, J., et al. 2015, ApJS, 221, 10
Bakker, E. J., van Dishoeck, E. F., Waters, L. B. F. M., & Schoenmaker, T. 1997, A&A, 323, 469
Benson, P. J., & Little-Marenin, I. R. 1987, ApJL, 316, L37
Blackman, E. G., Frank, A., Markiel, J. A., Thomas, J. H., & Van Horn, H. M. 2001, Natur, 409, 485
Bujarrabal, V., Gómez-González, J., Bachiller, R., & Martín-Pintado, J. 1988, A&A, 204, 242
Cernicharo, J., Guelin, M., Penalver, J., Martín-Pintado, J., & Mauersberger, R. 1989, A&A, 222, L1
Cerrigone, L., Trigilio, C., Umana, G., Buemi, C. S., & Leto, P. 2011, MNRAS, 412, 1137
Cragg, D. M., Sobolev, A. M., & Godfrey, P. D. 2002, MNRAS, 331, 521
Deguchi, S., Kawabe, R., Ukita, N., et al. 1988, ApJ, 325, 795
Desmurs, J.-F. 2012, in IAU Symp. 287, Cosmic Masers—from OH to H0, ed. R. S. Booth, E. M. L. Humphreys, & W. H. T. Vlemmings (Cambridge: Cambridge Univ. Press), 217
Desmurs, J.-F., Baudry, A., Sivagnanam, P., et al. 2010, A&A, 520, A45
Desmurs, J.-F., Baudry, A., Sivagnanam, P., & Henkel, C. 2002, A&A, 394, 975
Dinh-V-Trung, & Lim, J. 2008, ApJ, 678, 303
Dinh-V-Trung, & Rieu, N.-Q. 2000, A&A, 361, 601
Elitzur, M., & Asensio Ramos, A. 2006, MNRAS, 365, 779
Ellingsen, S. P., Cragg, D. M., Lovell, J. E. J., et al. 2004, MNRAS, 354, 401
Engels, D. 1994, A&A, 285, 497
Engels, D., Schmid-Burgk, J., Walmsley, C. M., & Winnberg, A. 1985, A&A, 148, 344
Etoka, S., Gérard, E., Richards, A. M. S., et al. 2017, MNRAS, 468, 1703
Etoka, S., & Le Squeren, A. M. 1997, A&A, 321, 877
Ford, K. E. S., Neufeld, D. A., Goldsmith, P. F., & Melnick, G. J. 2003, ApJ, 589, 430
García-Segura, G., Langer, N., Różyczka, M., & Franco, J. 1999, ApJ, 517, 767
García-Segura, G., Villaver, E., Langer, N., Yoon, S.-C., & Manchado, A. 2014, ApJ, 783, 74
Gómez, J. F., Uscanga, L., Green, J. A., et al. 2016, MNRAS, 461, 3259
Gómez, Y., Tafoya, D., Anglada, G., et al. 2009, ApJ, 695, 930
Gray, M. (ed.) 2012, Maser Sources in Astrophysics (Cambridge: Cambridge Univ. Press)
Habing, H. J. 1996, A&ARv, 7, 97
Herpin, F., & Cernicharo, J. 2000, ApJL, 530, L129
Herpin, F., Goicoechea, J. R., Pardo, J. R., & Cernicharo, J. 2001, in ESA Special Publication 460, The Promise of the Herschel Space Observatory, ed. G. L. Pilbratt et al. (Madrid: ESA), 249
Izumiura, H., Ukita, N., & Tsuji, T. 1995, ApJ, 440, 728
Kwok, S., & Feldman, P. A. 1981, ApJL, 247, L67
Lee, C.-F., Yang, C.-H., Sahai, R., & Sánchez Contreras, C. 2013, ApJ, 770, 153
Likkel, L., & Morris, M. 1988, ApJ, 329, 914
Likkel, L., Morris, M., & Maddalena, R. J. 1992, A&A, 256, 581
Little-Marenin, I. R., Benson, P. J., & Dickinson, D. F. 1988, ApJ, 330, 828
Little-Marenin, I. R., Sahai, R., Wannier, P. G., et al. 1994, A&A, 281, 451
Lucas, R., Guillotaeu, S., & Omont, A. 1988, A&A, 194, 230
Marschall, R., Su, C. C., Liao, Y., et al. 2016, A&A, 589, A90
Martín-Pintado, J., Bujarrabal, V., Bachiller, R., Gómez-González, J., & Planesas, P. 1988, A&A, 197, L15
Matthews, L. D., & Claussen, M. J. 2018, in ASP Conf. Ser. 517, Science with a Next Generation Very Large Array, ed. E. Murphy (San Francisco, CA: ASP), 281
Matthews, L. D., & Reid, M. J. 2007, AJ, 133, 2291
Melnick, G. J., Neufeld, D. A., Ford, K. E. S., Hollenbach, D. J., & Ashby, M. L. N. 2001, Natur, 412, 160
Miranda, L. F., Torrelles, J. M., Guerrero, M. A., Aaquist, O. B., & Eiroa, C. 1998, MNRAS, 298, 243
Nakada, Y., Izumiura, H., Onaka, T., et al. 1987, ApJL, 323, L77
Neufeld, D. A., & Dalgarno, A. 1989, ApJ, 340, 869
Nguyen-Q-Rieu, Bujarrabal, V., Olofsson, H., Johansson, L. E. B., & Turner, B. E. 1984, ApJ, 286, 276
Ohnaka, K., Boboltz, D. A., Mulitz-Schimel, G., Izumiura, H., & Wittkowski, M. 2013, A&A, 559, A120
Pardo, J. R., Cernicharo, J., Goicoechea, J. R., & Phillips, T. G. 2004, ApJ, 615, 495
Pavlakis, K. G., & Kylafis, N. D. 1996, ApJ, 467, 309
Pihlström, Y. M., Fish, V. L., Sjouwerman, L. O., et al. 2008, ApJ, 676, 371
Qiao, H.-H., Walsh, A. J., Gómez, J. F., et al. 2016, ApJ, 817, 37
Richards, A. M. S., Elitzur, M., & Yates, J. A. 2011, A&A, 525, A56
Sahai, R., & Patel, N. A. 2015, ApJL, 810, L8
Sánchez Contreras, C., Báez-Rubio, A., Alcolea, J., Bujarrabal, V., & Martín-Pintado, J. 2017, A&A, 603, A67
Sánchez Contreras, C., Bujarrabal, V., Castro-Carrizo, A., Alcolea, J., & Sargent, A. 2004, ApJ, 617, 1142
Schilke, P., & Menten, K. M. 2003, ApJ, 583, 446
Silverglate, P., Terzian, Y., Zuckerman, B., & Wolff, M. 1979, AJ, 84, 345
Sjouwerman, L. O., Fish, V. L., Claussen, M. J., Pihlström, Y. M., & Zschaechner, L. K. 2007, ApJL, 666, L101
Slijkhuis, S., Hu, J. Y., & de Jong, T. 1991, A&A, 248, 547
Stern, S. A., Shull, J. M., & Brandt, J. C. 1990, Natur, 345, 305
Strack, A., Araya, E. D., Lebrón, M. E., et al. 2018, in IAU Symp. 336, Astrophysical Masers: Unlocking the Mysteries of the Universe, ed. A. Tarchi, M. J. Reid, & P. Castangia (Cambridge: Cambridge Univ. Press), 385
Szczerba, R., Chen, P. S., Szymczak, M., & Omont, A. 2002, A&A, 381, 491
Szczerba, R., Schmidt, M. R., & Pulecka, M. 2007, BaltA, 16, 134
Szczerba, R., Szymczak, M., Babkovskaia, N., et al. 2006, A&A, 452, 561
Tafoya, D., Loinard, L., Fonfría, J. P., et al. 2013, A&A, 556, A35
te Lintel Hekkert, P. 1991, A&A, 248, 209
te Lintel Hekkert, P., Caswell, J. L., Habing, H. J., et al. 1991, A&AS, 90, 327
te Lintel Hekkert, P., & Chapman, J. M. 1996, A&AS, 119, 459
te Lintel Hekkert, P., Habing, H. J., Caswell, J. L., Norris, R. P., & Haynes, R. F. 1988, A&A, 202, L19
Thaddeus, P. 1972, ApJ, 173, 317
Trammell, S. R., & Goodrich, R. W. 2002, ApJ, 579, 688
Uscanga, L., Gómez, J. F., Suárez, O., & Miranda, L. F. 2012, A&A, 547, A40
Wyrowski, F., Schilke, P., Thorwirth, S., Menten, K. M., & Winnewisser, G. 2003, ApJ, 586, 344
Yoon, D.-H., Cho, S.-H, Kim, J., Yun, Y. J., & Park, Y.-S. 2014, ApJS, 211, 15
Zijlstra, A. A., Gaylard, M. J., te Lintel Hekkert, P., et al. 1991, A&A, 243, L9